

Neutron stars are too cool for simple wave-function collapse models

Antoine Tilloy^{1,*} and Thomas M. Stace²

¹Max-Planck-Institut für Quantenoptik, Hans-Kopfermann-Straße 1, 85748 Garching, Germany

²ARC Centre for Engineered Quantum Systems, School of Mathematics and Physics,
The University of Queensland, Brisbane, QLD 4072, Australia

Collapse models, like the Continuous Spontaneous Localization (CSL) model [1, 2], aim at solving the measurement problem of quantum mechanics through a stochastic non-linear modification of the Schrödinger equation [3, 4]. Such modifications have sometimes been conjectured to be caused by gravity, the most famous example being the Diósi-Penrose (DP) model [5, 6]. In general, collapse models posit an intrinsic (possibly gravitational) noise, which endogenously collapses superpositions of sufficiently macroscopic systems (in a particular basis), while preserving the predictions of quantum mechanics at small scales. One notable consequence of these models is spontaneous heating of massive objects. Neutron stars, which represent a stable state of matter that balances gravitational attraction with the Pauli exclusion principle, are extremely dense, macroscopic quantum-limited objects. As such, they offer a unique system on which to test the predictions of collapse models. Here, we calculate an estimate of the equilibrium temperature of a neutron star radiating heat generated from spontaneous collapse models. We find that the CSL model would result in equilibrium temperatures much higher than those observed in astrophysical neutron stars, ruling out all plausible CSL model parameter values. For the DP model, our calculation yields a bound on the model parameter.

Collapse models – Collapse models modify the Schrödinger equation with a non-linear noise term:

$$\partial_t |\psi_t\rangle = -\frac{i}{\hbar} H |\psi_t\rangle + F(\eta_t, |\psi_t\rangle) \quad (1)$$

where η_t is a white noise process and F some function which is partially constrained by consistency conditions [7, 8], and is chosen to yield a collapse in the position basis.

Although this stochastic description of the state vector is required to understand why collapse models actually achieve their purpose and solve the measurement problem, their empirical content is fully contained in the master equation obeyed by $\rho_t = \mathbb{E}[|\psi_t\rangle\langle\psi_t|]$. For *most* Markovian non-dissipative collapse models proposed so

far [8], it takes the form $\partial_t \rho_t = -\frac{i}{\hbar} [H, \rho_t] + \mathcal{D}[\hat{M}] \rho_t$ with

$$\mathcal{D}[\hat{M}] \rho = -\int d\mathbf{x} d\mathbf{y} f(\mathbf{x} - \mathbf{y}) \left[\hat{M}_{r_c}(\mathbf{x}), \left[\hat{M}_{r_c}(\mathbf{y}), \rho \right] \right] \quad (2)$$

where f is a positive definite function and $\hat{M}_{r_c}(\mathbf{x})$ is a regularized mass density operator:

$$\hat{M}_{r_c}(\mathbf{x}) = g_{r_c} * \hat{M}(\mathbf{x}) = g_{r_c} * \sum_{k=1}^n m_k a_k^\dagger(\mathbf{x}) a_k(\mathbf{x}). \quad (3)$$

In this expression, n is the number of particle species, m_k the mass of species k , $a_k^\dagger(\mathbf{x}), a_k(\mathbf{x})$ denote the usual fermionic or bosonic creation and annihilation operators for particles of type k in \mathbf{x} , and g_{r_c} is a regulator which smooths the mass density over a length scale r_c . Typically, the regulator function is taken to be Gaussian:

$$g_{r_c}(\mathbf{x}) = e^{-\mathbf{x}^2/(2r_c^2)} / (\sqrt{2\pi r_c^2})^3. \quad (4)$$

The regulator length scale has to be much larger than the Planck length and even the nucleon Compton wavelength, the usual choice being $r_c \simeq 10^{-7} \text{m}$ [9].

The two most common continuous collapse models are the Continuous Spontaneous Localization (CSL) model and the Diósi-Penrose model (the latter having a heuristic link with gravity):

1. The CSL model is obtained for:

$$f^{\text{CSL}}(\mathbf{x} - \mathbf{y}) = \frac{\gamma}{2m_N^2} \times \delta(\mathbf{x} - \mathbf{y}) \quad (5)$$

where m_N is the mass of a nucleon and γ is the collapse “strength”. It is a rate \times distance³. The corresponding rate is often taken to be $\lambda_{\text{CSL}} \equiv \gamma/(4\pi r_c^2)^{3/2} \simeq 10^{-16} \text{s}^{-1}$ [9].

2. The DP model is obtained for:

$$f^{\text{DP}}(\mathbf{x} - \mathbf{y}) = \frac{G}{4\hbar} \times \frac{1}{|\mathbf{x} - \mathbf{y}|}. \quad (6)$$

Because the collapse strength is fixed by the gravitational constant, there is one parameter less [10]. A modern motivation for eq. (6) is given by attempts at constructing models of fundamentally semiclassical gravity [11, 12].

The additional decoherence term eq. (2) in the master equation does not commute with the Hamiltonian, hence the expectation of the energy $\langle H \rangle_t \equiv \text{tr}[H \rho_t]$ is no longer conserved. Rather, because \hat{M} in eq. (3) is derived from

* antoine.tilloy@mpq.mpg.de

a classical white noise source, it corresponds to heating from a weakly coupled infinite temperature heat bath. This spontaneous heating provides a natural test of collapse models [13–15].

Recent proposals to test these models exploited have been built around ultra cold atoms [16], which may provide good platforms for to obtain bounds on the parameters in the theory as the heating effect should be significant in relative terms. An alternative, which has been overlooked so far, is to consider instead maximally dense systems, exploiting the mass density dependence of the heating for all collapse models. In this respect, neutron stars are ideal candidates.

Neutron star cooling has been studied theoretically and observationally. At early stages when $T_{\text{star}} \sim 10^9$ K, they cool by various baryonic emission processes, but at later stages, when $T_{\text{star}} \sim 10^6$ K or colder, the cooling is radiation dominated [17–19]. Thus, the equilibrium temperature is attained by the balance of the CSL heating with Stefan-Boltzmann radiation, so is determined by the heat balance condition $P_{\text{heat}} = P_{\text{rad}}$, where

$$P_{\text{heat}} = \partial_t \langle H \rangle_t = \text{tr}[H \mathcal{D}[\hat{M}]\rho_t] \quad (7)$$

and

$$P_{\text{rad}} = S\sigma T^4 \quad (8)$$

where S is the neutron star surface area and $\sigma = 5.6 \cdot 10^{-8} \text{W} \cdot \text{m}^{-2} \cdot \text{K}^{-4}$ is Stefan’s constant. It follows that at equilibrium $T_{\text{star}} = (P_{\text{heat}}/(S\sigma))^{1/4}$.

Neutron star model – We consider a crude model of a neutron star: a non-relativistic Fermi gas of neutrons in a $L \times L \times L$ cubic box. We take the typical neutron star length scale $L \sim 10$ km and mass $M_{\text{star}} \sim M_{\odot} \simeq 2.0 \cdot 10^{30}$ kg (hence $N_N = M_{\text{star}}/m_N \simeq 10^{57}$ neutrons).

The Fermi energy E_F of this system is

$$E_F = \frac{\hbar^2}{2m_N} \left(\frac{3\pi^2 N_N}{L^3} \right)^{2/3} \simeq 3 \cdot 10^{-11} \text{J} \simeq 200 \text{MeV}. \quad (9)$$

The corresponding Fermi temperature $T_F > 10$ GK is much larger than the observed temperatures $T_{\text{star}} < 1$ MK of the coldest known neutron stars. We shall thus assume that the neutron Fermi sea is in the ground state $|N\rangle$ to get an estimate on P_{heat} .

Intrinsic Heating Power – We now calculate the intrinsic heating power due to hypothetical continuous collapse processes. We proceed by computing P_{heat} for a degenerate, non-interacting Fermi gas consisting of N_N neutrons.

In the Fermi gas approximation, the star Hamiltonian is

$$H = \sum_{\mathbf{k}} E_{\mathbf{k}} b_{\mathbf{k}}^{\dagger} b_{\mathbf{k}} \quad (10)$$

where $\{b_{\mathbf{k}}^{\dagger}, b_{\mathbf{k}'}\} = \delta_{\mathbf{k}, \mathbf{k}'}$. The modefunctions and energies for a particle in the interior of a box (i.e. a ‘cubic star’)

of size $L \times L \times L$ are

$$\psi_{\mathbf{k}}(\mathbf{x}) = \left(\frac{2}{L}\right)^{3/2} \sin(k_x x) \sin(k_y y) \sin(k_z z), \quad (11)$$

$$E_{\mathbf{k}} = \frac{\hbar^2}{2m_N} \mathbf{k}^2, \quad (12)$$

where $\mathbf{k} = \pi \mathbf{n}/L$ with $\mathbf{n} = (n_x, n_y, n_z) \in (\mathbb{N}^*)^3$. Hence, the mode creation operators are related to the usual position-localised creation operators by

$$b_{\mathbf{k}}^{\dagger} = \int_{[0, L]^3} d\mathbf{x} \psi_{\mathbf{k}}(\mathbf{x}) a^{\dagger}(\mathbf{x}) \quad (13)$$

$$a^{\dagger}(\mathbf{x})|_{\text{inside box}} = \sum_{n_x, n_y, n_z=1}^{+\infty} \psi_{\mathbf{k}}(\mathbf{x}) b_{\mathbf{k}}^{\dagger}. \quad (14)$$

In terms of b ’s in eq. (2), and using eq. (7) we get

$$\begin{aligned} P_{\text{heat}} = & -m_N^2 \sum_{\mathbf{k}, \mathbf{k}_1, \mathbf{k}_2, \mathbf{k}_3, \mathbf{k}_4} E_{\mathbf{k}} \int d\mathbf{x} d\mathbf{y} g_{r_c} * f * g_{r_c}(\mathbf{x} - \mathbf{y}) \\ & \times \psi_{\mathbf{k}_1}(\mathbf{x}) \psi_{\mathbf{k}_2}(\mathbf{x}) \psi_{\mathbf{k}_3}(\mathbf{y}) \psi_{\mathbf{k}_4}(\mathbf{y}) \\ & \times \langle N | \left[b_{\mathbf{k}_1}^{\dagger} b_{\mathbf{k}_2}, \left[b_{\mathbf{k}_3}^{\dagger} b_{\mathbf{k}_4}, b_{\mathbf{k}}^{\dagger} b_{\mathbf{k}} \right] \right] | N \rangle \end{aligned} \quad (15)$$

where $|N\rangle$ is the ground state of the Fermi sea. The expectation value is easily evaluated using $[b_{\mathbf{k}_1}^{\dagger} b_{\mathbf{k}_2}, b_{\mathbf{k}_3}^{\dagger} b_{\mathbf{k}_4}] = \delta_{k_2 k_3} b_{\mathbf{k}_1}^{\dagger} b_{\mathbf{k}_4} - \delta_{k_1 k_4} b_{\mathbf{k}_3}^{\dagger} b_{\mathbf{k}_2}$, so that

$$\begin{aligned} \langle N | \left[b_{\mathbf{k}_1}^{\dagger} b_{\mathbf{k}_2}, \left[b_{\mathbf{k}_3}^{\dagger} b_{\mathbf{k}_4}, b_{\mathbf{k}}^{\dagger} b_{\mathbf{k}} \right] \right] | N \rangle = \\ \delta_{k_4 k} \delta_{k_2 k_3} \delta_{k_1 k} (\theta_{k_F - k} - \theta_{k_F - k_2}) \\ + \delta_{k k_3} \delta_{k_2 k} \delta_{k_1 k_4} (\theta_{k_F - k} - \theta_{k_F - k_1}) \end{aligned} \quad (16)$$

where θ_x is the Heaviside function. Taking into account the (so far neglected) spin degeneracy we find:

$$P_{\text{heat}} = 4 m_N^2 \sum_{|\mathbf{k}| > k_f} \sum_{|\mathbf{k}'| < k_f} (E_{\mathbf{k}} - E_{\mathbf{k}'}) \mathcal{F}(\mathbf{k}, \mathbf{k}'), \quad (17)$$

where $k_F = \pi n_F/L$ with $n_F = (3N_N/\pi)^{1/3}$, and \mathcal{F} is given by

$$\mathcal{F}(\mathbf{k}, \mathbf{k}') = \int_{V^2} d\mathbf{x} d\mathbf{x}' f_{r_c}(\mathbf{x} - \mathbf{x}') \psi_{\mathbf{k}}(\mathbf{x}) \psi_{\mathbf{k}}(\mathbf{x}') \psi_{\mathbf{k}'}(\mathbf{x}) \psi_{\mathbf{k}'}(\mathbf{x}'), \quad (18)$$

where $f_{r_c} = g_{r_c} * f * g_{r_c} = f * g_{\sqrt{2}r_c}$ and $V = [0, L]^3$. Qualitatively, the function $\mathcal{F}(\mathbf{k}, \mathbf{k}')$ is approximately constant for $\kappa_{\pm} = |\mathbf{k} \pm \mathbf{k}'| < 1/r_c$, and cuts off quickly for $\kappa_{\pm} > 1/r_c$. We give an explicit expression for \mathcal{F} for both the CSL and DP models in supplementary material 2.

To get a more manageable form for eq. (17), we replace the sum by an integral

$$\sum_{\mathbf{n}} \rightarrow \int d^3 \mathbf{n} \quad (19)$$

We note that the argument of eq. (17) is exponentially small except near the Fermi surface, and since $k_F \sim$

10^{15} m^{-1} is extremely large compared to other scales, we find

$$\begin{aligned} P_{\text{heat}} &\simeq 4m_N^2 (4\pi)^2 \int_0^{n_F} n'^2 dn' \int_{n_F}^{+\infty} n^2 dn (E_n - E_{n'}) \mathcal{F}(n, n') \\ &\simeq 4m_N^2 (4\pi)^2 n_F^4 \int_0^{n_F} dn' \int_{n_F}^{+\infty} dn (E_n - E_{n'}) \mathcal{F}(n, n') \end{aligned} \quad (20)$$

The double integral can be evaluated using the fact that $k_F^{-1} \ll r_c$ (see supplementary material). For the CSL model we find

$$P_{\text{heat}}^{(\text{CSL})} = \frac{(4\pi)^2}{16\sqrt{\pi}} \frac{\gamma \hbar^2}{r_c^3 m_N L^2} n_F^5 \quad (21)$$

$$= \frac{3^{5/3}}{2\pi^{2/3}} \frac{\lambda \hbar^2}{m_N L^2} N_N^{5/3} \quad (22)$$

$$\sim \frac{G^2 m_N^5}{\hbar^2} \gamma \frac{N_N^{7/3}}{r_c^3}, \quad (23)$$

where the last term expresses the heating power in fundamental units (including the CSL parameters γ and r_c), based on the estimate $L = R_{\text{star}} \approx \hbar^2 / (Gm_N^3 N_N^{1/3})$ given in eq. (28) (and neglecting numerical prefactors of order unity). Importantly, $P_{\text{heat}}^{(\text{CSL})}$ grows superlinearly with the mass of the star, and inversely with the surface area. The superlinear scaling in N_N is what makes neutron stars a good platform to test the CSL model compared with bulk matter where the radiated power is additive in the number of particles.

For $\lambda = 10^{-16} \text{ s}^{-1}$, the historical GRW value, we find $P_{\text{heat}}^{(\text{CSL})} \sim 10^{30} \text{ W}$, which is several orders of magnitude greater than our own sun. Using the Stefan-Boltzmann formula, this corresponds to a surface temperature $T_{\text{star}}^{(\text{CSL})} \sim 10 \text{ MK}$. This figure is a factor of 30 times hotter than the coldest observed neutron stars [20], $T_{\text{star}}^{(\text{obs})} \sim 0.3 \text{ MK}$. Given that P_{rad} is a rapidly increasing function of T_{star} , the observed neutron star temperatures rule out the conventional GRW values.

Performing the same calculation for the DP model we find

$$P_{\text{heat}}^{(\text{DP})} = 2\sqrt{\pi} \frac{G \hbar m_N}{r_c^3} n_F^3 = \frac{6}{\sqrt{\pi}} G \hbar m_N \frac{N_N}{r_c^3}. \quad (24)$$

The heating power for the DP model grows only linearly in the number of neutrons, and does not depend explicitly on the star diameter but depends sensitively on the smoothing length, r_c . Taking r_c of the order of the proton radius, $r_c \sim 10^{-15} \text{ m}$, sometimes suggested as natural cutoff for the DP model, gives the same radiated power ($\sim 10^{30} \text{ W}$) and equilibrium temperature ($\sim 10^7 \text{ K}$) as before, and is therefore ruled out by observations. In general, $r_c \lesssim 10^{-14} \text{ m}$ is ruled out for the DP model.

Discussion – The lowest observed temperature of an astronomical neutron star is $T_{\text{star}}^{(\text{obs})} = 0.28 \text{ MK}$ for the object PSR J 840-1419 [20]. We note that neutron star

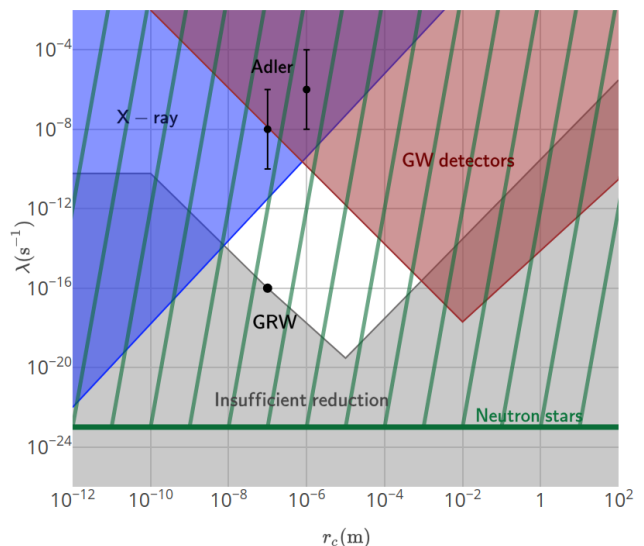


FIG. 1. CSL parameter diagram – Top: Zones formerly excluded by gravitational wave detectors [21, 22] (red), spontaneous X-ray emission [23] (blue), and insufficient macroscopic localization [24]. The white diamond represents the values still allowed before the present work. The value historically proposed by GRW [9] and the range put forward by Adler [25] are shown with black dots. The new region (hashed in green) up to $\lambda \gtrsim 10^{-23} \text{ s}^{-1}$ is excluded by the existence of cold neutron stars. Neutron star observations exclude the previously allowed white diamond, and together with the region of insufficient reduction, rule out the CSL model.

masses typically fall within a narrow range, so that the observed minimum temperature is expected to occur in the time-line for all neutron star cooling histories. The observed temperature corresponds to a radiative dissipation rate of $P_{\text{rad}}^{(\text{obs})} = 10^{26} \text{ W}$.

We now discuss how this observation constrains feasible values of parameters λ, r_c in the CSL and DP models, assuming solar mass neutron stars.

For the CSL model, using eq. (22), the radiated power from PSR J 840-1419 gives an upper bound on the CSL coupling parameter $\lambda \lesssim 10^{-23} \text{ s}^{-1}$.

In contrast, to provide sufficient decoherence to suppress macroscopic superpositions (e.g. the smallest visible object, $\sim 10 \mu\text{m}$, should become localized faster than the biological perception time of the eye $\sim 10 \text{ ms}$ [24]), requires $\lambda \gtrsim 10^{-19} \text{ s}^{-1}$. Thus, the upper bound determined by the observed neutron star is substantially lower than the lower bound required for the CSL to provide non-trivial collapse. We thus conclude that the CSL model is, in practical terms, ruled out (see Fig. 1).

Naturally, the theoretical lower bound is not sharp. Weaker conditions on λ could be obtained with weaker localization requirements, e.g. that measurement results printed on paper are well localized [26]. In our opinion, such constraints are extremely contrived. Similarly, extensions of the CSL model with colored noise (cCSL) [27, 28], dissipation (dCSL) [29], or both [30], containing

additional parameters (such as a high frequency cutoff or a temperature) are known to yield weaker heating effects and thus may evade the conclusions we put forward here.

For the DP model, small values of r_c are constrained by the heating rate we computed, but large values are also prohibited when the DP model is taken as a candidate for fundamentally semiclassical gravity [12]. In this context, the decoherence regularization affects the Newtonian potential and the $1/r^2$ law of the gravitational force breaks down for $r \sim r_c$. The Newtonian force is well measured for distances as short as $100\mu\text{m}$, which provides a conservative upper bound for r_c . For $T_{\text{star}}^{(\text{obs})}$ we get $r_c \gtrsim 10^{-14}\text{m}$, hence for the DP model ($10^{-14}\text{m} \lesssim r_c \lesssim 10^{-4}\text{m}$) remains an admissible range of the smoothing parameter for the theory. Note that the lower bound is of the same order of magnitude as the constraint from gravitational wave detectors [22]. We note that new observations of lower $T_{\text{star}}^{(\text{obs})}$ would further constrain the lower bound on r_c .

The analysis presented in this paper makes ‘lumped-element’ approximations that provide robust bounds on the radiated power. For example, we have assumed that the emissivity of a neutron star is unity, that the mass density is uniform, and that the thermal conductivity throughout the core is large enough that the star temper-

ature is approximately uniform. If these assumptions are relaxed, then the core temperature may be substantially higher than the observed surface temperature. Neutron superfluidity [18] has been hypothesised in the core of neutron stars. This phase will have a corresponding critical temperature T_c , which may provide a sensitive thermometric bound on tolerable heat generation rates in the star core: superfluidity will be suppressed if the internal temperature is too high. More generally, heat transfer models that include realistic constitutive models for the neutron star body may thus be able to provide even more stringent bounds on collapse model parameters than the lumped-element approximations we have adopted here.

In summary, our analysis of the heating of neutron stars attributable to spontaneous collapse indeed falsifies the CSL model, and provides a constraint on the DP model. Future observations of cold neutron stars, along with more sophisticated heat transfer models, will further constrain feasible parameters in the collapse models, including gravitationally motivated ones.

Acknowledgments – We thank T. Guaita for comments. AT was supported by the Alexander von Humboldt foundation. TMS was supported by the Australian Research Council Centre of Excellence for Engineered Quantum Systems (Grant No. CE 110001013).

-
- [1] P. Pearle, *Phys. Rev. A* **39**, 2277 (1989).
 [2] G. C. Ghirardi, P. Pearle, and A. Rimini, *Phys. Rev. A* **42**, 78 (1990).
 [3] A. Bassi and G. Ghirardi, *Phys. Rep.* **379**, 257 (2003).
 [4] A. Bassi, K. Lochan, S. Satin, T. P. Singh, and H. Ubricht, *Rev. Mod. Phys.* **85**, 471 (2013).
 [5] L. Diósi, *Phys. Lett. A* **120**, 377 (1987).
 [6] R. Penrose, *Gen. Relativ. Gravit.* **28**, 581 (1996).
 [7] N. Gisin, *Helv. Phys. Acta* **62**, 363 (1989).
 [8] A. Bassi, D. Dürr, and G. Hinrichs, *Phys. Rev. Lett.* **111**, 210401 (2013).
 [9] G. C. Ghirardi, A. Rimini, and T. Weber, *Phys. Rev. D* **34**, 470 (1986).
 [10] Note that the factor 1/4 in eq. (6) has also been fixed to 1/8 in the literature.
 [11] A. Tilloy and L. Diósi, *Phys. Rev. D* **93**, 024026 (2016).
 [12] A. Tilloy and L. Diósi, *Phys. Rev. D* **96**, 104045 (2017).
 [13] P. Pearle and E. Squires, *Phys. Rev. Lett.* **73**, 1 (1994).
 [14] M. Bahrami, *Phys. Rev. A* **97**, 052118 (2018).
 [15] S. L. Adler and A. Vinante, *Phys. Rev. A* **97**, 052119 (2018).
 [16] F. Laloë, W. J. Mullin, and P. Pearle, *Phys. Rev. A* **90**, 052119 (2014).
 [17] J. M. Lattimer, K. A. van Riper, M. Prakash, and M. Prakash, *Astrophysical Journal* **425**, 802 (1994).
 [18] J. M. Lattimer and M. Prakash, *The Astrophysical Journal* **550**, 426 (2001).
 [19] D. Yakovlev and C. Pethick, *Annual Review of Astronomy and Astrophysics* **42**, 169 (2004), <https://doi.org/10.1146/annurev.astro.42.053102.134013>.
 [20] E. F. Keane, M. A. McLaughlin, M. Kramer, B. W. Stappers, C. G. Bassa, M. B. Purver, and P. Weltevrede, *ApJ* **764**, 180 (2013).
 [21] M. Carlesso, A. Bassi, P. Falferi, and A. Vinante, *Phys. Rev. D* **94**, 124036 (2016).
 [22] B. Helou, B. J. J. Slagmolen, D. E. McClelland, and Y. Chen, *Phys. Rev. D* **95**, 084054 (2017).
 [23] K. Piscicchia, A. Bassi, C. Curceanu, R. D. Grande, S. Donadi, B. C. Hiesmayr, and A. Pichler, *Entropy* **19**, 7 (2017).
 [24] M. Toros, G. Gasbarri, and A. Bassi, *Phys. Lett. A* **381**, 3921 (2017).
 [25] S. L. Adler, *J. Phys. A: Math. Theor.* **40**, 2935 (2007).
 [26] W. Feldmann and R. Tumulka, *J. Phys. A: Math. Theor.* **45**, 065304 (2012).
 [27] A. Bassi and G. Ghirardi, *Phys. Rev. A* **65**, 042114 (2002).
 [28] S. L. Adler and A. Bassi, *J. Phys. A: Math. Theor.* **40**, 15083 (2007).
 [29] A. Smirne, B. Vacchini, and A. Bassi, *Phys. Rev. A* **90**, 062135 (2014).
 [30] L. Ferialdi and A. Bassi, *Phys. Rev. A* **86**, 022108 (2012).

SUPPLEMENTARY MATERIAL

1. Neutron star model

Our objective here is to derive an estimate of a neutron star radius R_{star} and Fermi energy starting with a simple model. We aim to demonstrate that the approximate values we use in the main text are robust and can be obtained even from a crude non-relativistic modeling. To simplify the calculation, we assume the neutron superfluid has uniform density. We proceed by finding a value of R that minimises the total quantum mechanical energy of non-interacting fermionic neutrons constituting the star.

On the interior of spherically symmetric star with a uniform mass distribution, the gravitational potential is harmonic

$$V(r) = -V_0 + m_N \omega^2 r^2 / 2, \quad (25)$$

where $V_0 = 3GM_{\text{star}}m_N/(2R) = 3GN_Nm_N^2/(2R)$, $N_N = M_{\text{star}}/m_N$ is the total number of neutrons in the star, and $\omega^2 = GM_{\text{star}}/R^3$. V_0 is chosen so that the interior potential matches to the $1/r$ exterior potential, which vanishes as $r \rightarrow \infty$, i.e. V_0 is the gravitational binding energy of a particle at $r = 0$.

The single particle eigenenergies of this potential are $E_{n,l,m} = E_n = \hbar\omega(n + 3/2) - V_0$, where n is the principle quantum number, l is the angular momentum quantum number, and m is the z -projection quantum number. The degeneracy of each eigenenergy is $l = 0, 2, 4, \dots, n$ if n is even or $l = 1, 3, 5, \dots, n$ if n is odd. As usual, $m = -l, \dots, l-1, l$. It is easy to check that the degeneracy of level n is $d_n = 2 \times (1+n)(2+n)/2$, and we include the factor of 2 to account for spin.

Filling up the neutron Fermi sea up to the maximum principle quantum number n_F gives

$$N_N = \sum_{n=0}^{n_F} d_n \approx n_F^3/3, \quad (26)$$

so the principle number at the Fermi surface is $n_F \approx (3N_N)^{1/3}$.

The total energy of the neutron Fermi sea is then

$$E_{\text{tot}} = \sum_{p=0}^{n_F} E_p d_p \approx \hbar\omega n_F^4/4 + n_F^3(2\hbar\omega - V_0/3) + O(n_F^2). \quad (27)$$

Since $\omega \sim R^{-3/2}$, and $V_0 \sim 1/R$, there is a minimum in E_{tot} as a function of R . This occurs at

$$R_{\text{star}} \sim \frac{9 \times 3^{2/3} n_F^2 \hbar^2}{16 G m_N^3 N_N} \sim \frac{9 \times 3^{2/3}}{4} \frac{\hbar^2}{G(m_N^8 M_{\text{star}})^{1/3}}. \quad (28)$$

Substituting for a solar mass ($M_{\text{star}} = 2 \times 10^{30}$ kg), and the other physical constants gives $R_{\text{star}} \sim 15$ km. We also find the harmonic trap frequency is $\omega \sim 60$ kHz, and the Fermi energy is $E_F = \hbar\omega n_F = 60$ MeV (which is about $T_F = 680$ GK).

We briefly note that our assumption of uniform mass density is not fully self-consistent, since the mass density of the fermions will not be somewhat greater near the core of the the star. However the estimates above are consistent with the typical values given for solar mass neutron stars, and so capture the essential gravitational binding physics.

In the main text, we perform calculations for gravitational heating assuming a ‘cubic star’ model, in which the neutrons are approximated as uniformly occupying a cube of side length $L \sim R_{\text{star}}$.

2. Computing \mathcal{F}

We evaluate $\mathcal{F}(\mathbf{k}, \mathbf{k}')$ eq. (18), using the shorthand $V = I^3 = [0, L]^3$ to indicate an integration volume. We have:

$$\mathcal{F}(\mathbf{k}, \mathbf{k}') = \int_{V^2} d\mathbf{x} d\mathbf{x}' f_{r_c}(\mathbf{x} - \mathbf{x}') \psi_{\mathbf{k}}(\mathbf{x}) \psi_{\mathbf{k}}(\mathbf{x}') \psi_{\mathbf{k}'}(\mathbf{x}) \psi_{\mathbf{k}'}(\mathbf{x}'), \quad (29)$$

$$= \int_{V^2} d\mathbf{x} d\mathbf{x}' \int_{\mathbb{R}^3} d\mathbf{x}'' f(\mathbf{x}'') g_{\bar{r}_c}(\mathbf{x} - \mathbf{x}' - \mathbf{x}'') \psi_{\mathbf{k}}(\mathbf{x}) \psi_{\mathbf{k}}(\mathbf{x}') \psi_{\mathbf{k}'}(\mathbf{x}) \psi_{\mathbf{k}'}(\mathbf{x}') \quad (30)$$

$$= \int_{\mathbb{R}^3} d\mathbf{x}'' f(\mathbf{x}'') \int_V d\mathbf{x}' \psi_{\mathbf{k}}(\mathbf{x}') \psi_{\mathbf{k}'}(\mathbf{x}') \underbrace{\int_V d\mathbf{x} g_{\bar{r}_c}(\mathbf{x} - \mathbf{x}' - \mathbf{x}'') \psi_{\mathbf{k}}(\mathbf{x}) \psi_{\mathbf{k}'}(\mathbf{x})}_{G(\mathbf{x}' + \mathbf{x}'')} \quad (31)$$

where $\tilde{r}_c = \sqrt{2}r_c$. The last line is useful because it tells us we can convolve the pseudo-density $\psi_{\mathbf{k}}(\mathbf{x})\psi_{\mathbf{k}'}(\mathbf{x})$ with the regularization kernel first, and then do the other integrals later, including for whichever choice is made for f . Defining $\tilde{\mathbf{x}} = \mathbf{x}' + \mathbf{x}''$, taking values in \mathbb{R}^3 , the last integral above becomes:

$$G(\tilde{\mathbf{x}}) = \int_V d\mathbf{x} g_{\tilde{r}_c}(\mathbf{x} - \tilde{\mathbf{x}}) \psi_{\mathbf{k}}(\mathbf{x})\psi_{\mathbf{k}'}(\mathbf{x}) \quad (32)$$

$$= \frac{1}{\left(\sqrt{2\pi\tilde{r}_c^2}\right)^3} \int_V d\mathbf{x} e^{-(\mathbf{x}-\tilde{\mathbf{x}})^2/(2\tilde{r}_c^2)} \psi_{\mathbf{k}}(\mathbf{x})\psi_{\mathbf{k}'}(\mathbf{x}) \quad (33)$$

$$= \frac{1}{\left(\sqrt{2\pi\tilde{r}_c^2}\right)^3} \left[\frac{2}{L}\right]^3 H_X(\tilde{x})H_Y(\tilde{y})H_Z(\tilde{z}) \quad (34)$$

where $H_X(\tilde{x}) \equiv \int_I dx e^{-(x-\tilde{x})^2/(2\tilde{r}_c^2)} \sin(k_x x) \sin(k'_x x)$ and equivalently for H_Y and H_Z . We use the identity $\sin(a)\sin(b) = \frac{1}{2}(\cos(a-b) - \cos(a+b))$ and the fact that $\tilde{r}_c \ll L$ to evaluate these integrals. We get that for $\tilde{x} \in [0, L]$:

$$H_X(\tilde{x}) \approx \int_{-\infty}^{\infty} dx e^{-(x-\tilde{x})^2/(2\tilde{r}_c^2)} \sin(k_x x) \sin(k'_x x) \quad (35)$$

$$= \sqrt{\frac{\pi}{2}} \tilde{r}_c \left(e^{-(k_x - k'_x)^2 \tilde{r}_c^2 / 2} \cos((k_x - k'_x)\tilde{x}) - e^{-(k_x + k'_x)^2 \tilde{r}_c^2 / 2} \cos((k_x + k'_x)\tilde{x}) \right), \quad (36)$$

This is a very accurate approximation because of the Gaussian regularization. For $\tilde{x} \notin [0, L]$, $H_X(\tilde{x}) \simeq 0$. The other integrals contributing to G can be evaluated similarly.

We will now carry the x component of the \mathbf{x}' integral in eq. (31):

$$K_X(x'') \equiv \int_I dx' \sin(k_x x') \sin(k'_x x') H_X(x' + x'') \quad (37)$$

$$= \int_{\max(0, -x'')}^{\min(L, L-x'')} dx' \sin(k_x x') \sin(k'_x x') H_X(x' + x'') \quad (38)$$

Linearizing all the trigonometric expressions and keeping only the (extensive) non-oscillatory terms yields:

$$K_X(x'') = \sqrt{\frac{\pi}{2}} \tilde{r}_c \frac{\max(0, L - |x''|)}{4} \left(e^{-(k_x - k'_x)^2 \tilde{r}_c^2 / 2} \cos((k_x - k'_x)x'') + e^{-(k_x + k'_x)^2 \tilde{r}_c^2 / 2} \cos((k_x + k'_x)x'') \right). \quad (39)$$

In the following, this function will be evaluated for arguments x'' much smaller than L (large momenta on the Fermi shell), hence the term $\max(0, L - |x''|)$ will be well approximated by L .

We now do the leftmost integral in eq. (31) over \mathbf{x}''

$$\mathcal{F}(\mathbf{k}, \mathbf{k}') = \frac{1}{\left(\sqrt{2\pi\tilde{r}_c^2}\right)^3} \left[\frac{2}{L}\right]^6 \int_{\mathbb{R}^3} d\mathbf{x}'' f(x'', y'', z'') K_X(x'') K_Y(y'') K_Z(z''). \quad (40)$$

For the CSL model, $f(\mathbf{x}'') \propto \delta(\mathbf{x}'')$ so the \mathbf{x}'' integral is now trivial:

$$\mathcal{F}_{\text{CSL}}(\mathbf{k}, \mathbf{k}') = \frac{1}{\left(\sqrt{2\pi\tilde{r}_c^2}\right)^3} \left[\frac{2}{L}\right]^6 \frac{\gamma}{m_N^2} K_X(0) K_Y(0) K_Z(0) \quad (41)$$

$$= \frac{1}{\left(\sqrt{2\pi\tilde{r}_c^2}\right)^3} \left[\frac{2}{L}\right]^6 \frac{\gamma}{m_N^2} \left(\sqrt{\pi} \frac{L\tilde{r}_c}{4\sqrt{2}} \right)^3 \sum_{\kappa=|k_x \pm k'_x, k_y \pm k'_y, k_z \pm k'_z|} e^{-\kappa^2 \tilde{r}_c^2 / 2} \quad (42)$$

$$= \frac{\gamma}{16m_N^2 L^3} \sum_{\kappa=|k_x \pm k'_x, k_y \pm k'_y, k_z \pm k'_z|} e^{-\kappa^2 \tilde{r}_c^2 / 2} \quad (43)$$

For the DP model, $f(\mathbf{x}'') \propto |\mathbf{x}''|^{-1}$ and the computation is a bit more tedious. One has:

$$\mathcal{F}_{\text{DP}}(\mathbf{k}, \mathbf{k}') = \frac{1}{\left(\sqrt{2\pi\tilde{r}_c^2}\right)^3} \left[\frac{2}{L}\right]^6 \frac{G}{4\hbar} \left(\sqrt{\frac{\pi}{2}} \frac{L\tilde{r}_c}{4} \right)^3 \sum_{\kappa=|k_x \pm k'_x, k_y \pm k'_y, k_z \pm k'_z|} J_{\kappa} e^{-\kappa^2 \tilde{r}_c^2 / 2} \quad (44)$$

where:

$$J_\kappa = \int_{\mathbb{R}^3} d\mathbf{x} \cos(\kappa_x x) \cos(\kappa_y y) \cos(\kappa_z z) \frac{\max(0, L - |\mathbf{x}''|)}{L|\mathbf{x}|} \quad (45)$$

$$\simeq \int_{\mathbb{R}^3} d\mathbf{x} \cos(\kappa_x x) \cos(\kappa_y y) \cos(\kappa_z z) / |\mathbf{x}|. \quad (46)$$

where the approximation comes from the fact that J_κ will be integrated for arguments $\kappa \gg L^{-1}$. We thus get:

$$J_\kappa \simeq \frac{1}{8} \sum_{\varepsilon_x, \varepsilon_y, \varepsilon_z = \pm 1} \int_{\mathbb{R}^3} d\mathbf{x} \frac{e^{i\kappa_\varepsilon \cdot \mathbf{x}}}{|\mathbf{x}|} \quad (47)$$

with $\kappa_\varepsilon = \{\kappa_x \varepsilon_x, \kappa_y \varepsilon_y, \kappa_z \varepsilon_z\}$. Hence

$$J_\kappa \simeq 4\pi \frac{1}{|\kappa|^2} \quad (48)$$

3. Computing the integral

Our objective is to compute

$$\mathcal{I} = \int_0^{n_F} dn' \int_{n_F}^{+\infty} dn [E_n - E_{n'}] \mathcal{F}(n, n') \quad (49)$$

for the CSL and DP models. We start with the CSL model.

$$\mathcal{I}_{\text{CSL}} = \frac{\hbar^2}{2m_N} \frac{\pi^2}{L^2} \frac{\gamma}{16m_N^2 L^3} \int_0^{n_F} dn' \int_{n_F}^{+\infty} dn [n^2 - n'^2] e^{-\pi^2(n-n')^2 \tilde{r}_c^2 / (2L^2)} \quad (50)$$

$$\simeq \frac{\hbar^2}{2m_N} \frac{\pi^2}{L^2} \frac{\gamma}{16m_N^2 L^3} 2n_F \int_0^{n_F} dn' \int_{n_F}^{+\infty} dn [n - n'] e^{-\pi^2(n-n')^2 \tilde{r}_c^2 / (2L^2)} \quad (51)$$

The integral can be computed using the change of variables:

$$\int_0^{n_{\text{max}}} dn \int_{n_{\text{max}}}^{+\infty} dn' (n - n') \exp \left[-\frac{\pi^2 \tilde{r}_c^2}{2L^2} |n - n'|^2 \right] = \int_0^{n_{\text{max}}} du \int_0^{+\infty} dv (u + v) \exp \left[-\frac{\pi^2 \tilde{r}_c^2}{2L^2} |u + v|^2 \right] \quad (52)$$

$$\simeq \int_0^{+\infty} du \int_0^{+\infty} dv (u + v) \exp \left[-\frac{\pi^2 \tilde{r}_c^2}{2L^2} |u + v|^2 \right] \quad (53)$$

$$= \frac{\sqrt{\pi}}{4} \left[\frac{2L^2}{\pi^2 \tilde{r}_c^2} \right]^{3/2} = \frac{\sqrt{2\pi} L^3}{2\pi^3 \tilde{r}_c^3} \quad (54)$$

Hence:

$$\mathcal{I}_{\text{CSL}} = 2 \frac{\sqrt{2\pi} L^3}{2\pi^3 \tilde{r}_c^3} \frac{\hbar^2}{2m_N} \frac{\pi^2}{L^2} \frac{\gamma}{16m_N^2 L^3} n_F = \frac{1}{64\sqrt{\pi}} \frac{\gamma \hbar^2}{r_c^3 m_N^3 L^2} n_F \quad (55)$$

For the DP model, we just have to introduce the J_κ term which removes 2 factors of n_f , and the non-trivial part of the computation reduces to evaluating the integral eq. (54). It yields:

$$\mathcal{I}_{\text{DP}} = 2 \frac{\sqrt{2\pi} L^3}{2\pi^3 \tilde{r}_c^3} \frac{\hbar^2}{2m_N} \frac{G}{32\hbar L^3} 4\pi n_F^{-1} = \frac{1}{32\pi^{3/2}} \frac{G\hbar}{m_N r_c^3} n_F^{-1} \quad (56)$$